# Supercavitating Body Dynamics, Bifurcations and Control

Guojian Lin, Balakumar Balachandran and Eyad Abed

*Abstract*— Numerical investigations conducted into the dive-plane dynamics of supercavitating bodies, which are described by a non-smooth system, are discussed. For a selected set of system-parameter values, a fundamental understanding of the solution structure obtained in terms of equilibrium and periodic solutions is presented. After carrying out smoothing approximations, bifurcations of solutions of the resulting smooth system are studied by using the cavitation number as a control parameter. Supercritical Hopf bifurcations of fixed points and period-doubling bifurcations are found, and the use of feedback control to suppress or delay the onset of Hopf bifurcation is presented. The present work provides a basis for interpreting the tail-slap phenomenon of a supercavitating body as a limit-cycle motion and controlling it.

## I. INTRODUCTION

Cavitation is the physical phenomena of bubble formation in a liquid subject to local pressure variations. The cavitation number $\sigma$, which is used to characterize the extent of cavitation, is defined as

$$\sigma = \frac{p_\infty - p_c}{0.5\rho V^2} \tag{1}$$

where $\rho$ is the fluid density, $V$ is the vehicle velocity, $p_\infty$ and $p_c$ are respectively the ambient pressure and the cavity pressure. Supercavitation, which is an extreme form of cavitation in which a single bubble envelops the moving vehicle almost completely (see Fig. 1), corresponds to very small values of the cavitation number [1], [2]. Due to the reduced drag forces associated with a supercavitating body, dramatic increases can be realized in the speed of supercavitating body [1], [2], [3]. However, supercavitation involves complicated cavity dynamics, the body experiences strong nonlinear forces, and the system dynamics presents challenges to stabilization, control, and maneuvering of the body [2].

Dive plane dynamics and control of underwater vehicles are studied in the references [1] and [4]. In the study [1], a stable limit cycle of supercavitating vehicle is found, a nonlinear control law is designed to cancel the planing force and the resulting system is a stable linear system. The change of system dynamics as parameters vary is not considered though. In the study [4], a supercritical pitch

G. Lin is a graduate research assistant in the Department of Electrical and Computer Engineering, University of Maryland, College Park, MD. 20742. linguoji@eng.umd.edu

B. Balachandran is a Professor in the Department of Mechanical Engineering, University of Maryland, College Park, MD 20742. balab@eng.umd.edu

E. Abed is a Professor in the Department of Electrical and Computer Engineering, University of Maryland, College Park, MD 20742. abed@eng.umd.edu
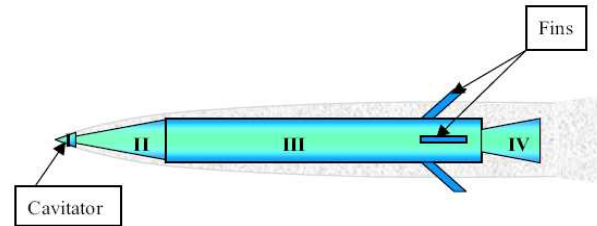
Fig. 1. A supercavitating body with an envelope surrounding it.

fork bifurcation is found in the dynamics of an underwater submersible vehicle with respect to the forward cruising speed and different linear feedback control laws are applied to stabilize the system to the desired equilibria located on different sides of the critical point. The occurrence and the analysis of the pitch fork bifurcation is related to the fact that the buoyancy force cancels the gravity force in nominal conditions. For a supercavitating vehicle, however, the buoyancy force is very small and this force is omitted in most cases. On the other hand, the tail of the supercavitating body slaps the cavity wall under certain conditions and this tail-slap phenomenon complicates the system dynamics.

In previous work [3], the authors presented analysis of the equilibrium and limit-cycle solutions of the supercavitating system to construct a picture of the dynamics of the supercavitating body for a set of system parameters. The system was approximated as a piecewise linear system and switching feedback control was used to stabilize the original system to a desired equilibrium point. The current work is an extension of the previous work, and here, specific attention is paid to the bifurcations in the system with respect to the cavitation number. To carry out the bifurcation analysis, the non-smooth system is converted to a smooth system by using hypertangent functions, and this system is studied by using the continuation software AUTO97 [5]. The use of feedback control to delay the onset of Hopf bifurcations and suppression of these bifurcations is also studied here. The Hopf bifurcations can be helpful for understanding the tail-slap phenomenon, which is characterized by oscillations of the body into and out of the bubble.

The rest of the paper is organized as follows. In Section II, the dive-plane model of a supercavitating body is presented. Results illustrative of system dynamics are presented for a special cavitation number in Section III. Bifurcations determined with respect to the cavitation number are presented in Section IV. In Section V, control schemes that suppress or delay the bifurcations are discussed. Concluding remarks are collected in Section VI.

## II. GOVERNING EQUATIONS OF SUPERCAVITATING BODY

Following the work of Dzielski and Kurdila [1], a four-state model is chosen to study dive-plane dynamics and control of the system shown in Fig. 1. The forward velocity $V$ is assumed to be constant and the four states of this model are $z$ (the depth at which the body is located), $w$ (the vertical speed of the body), $\theta$ (the pitch angle), and $q$ (the pitch rate). This system has two control inputs, namely, the cavitator deflection angle $\delta_c$ and the elevator deflection angle $\delta_e$. This model takes into account the non-linear planing force, which is descriptive of the nonlinear interaction between the body and the cavity, and a simplified description of the cavity dynamics. The governing equations can be determined in a body-fixed reference frame as

$$
\begin{pmatrix} \dot{z} \\ \dot{w} \\ \dot{\theta} \\ \dot{q} \end{pmatrix} = \begin{pmatrix} 0 & 1 & -V & 0 \\ 0 & a_{22} & 0 & a_{24} \\ 0 & 0 & 0 & 1 \\ 0 & a_{42} & 0 & a_{44} \end{pmatrix} \begin{pmatrix} z \\ w \\ \theta \\ q \end{pmatrix}
$$
$$
+ \begin{pmatrix} 0 & 0 \\ b_{21} & b_{22} \\ 0 & 0 \\ b_{41} & b_{42} \end{pmatrix} \begin{pmatrix} \delta_e \\ \delta_c \end{pmatrix} + \begin{pmatrix} 0 \\ c_2 \\ 0 \\ 0 \end{pmatrix} \quad (2)
$$
$$
+ \begin{pmatrix} 0 \\ d_2 \\ 0 \\ d_4 \end{pmatrix} (-V^2[1-(\frac{R_c-R}{h'R+R_c-R})^2]\frac{1+h'}{1+2h'}\alpha)
$$

The term $c_2$ and the last two terms in Eq. (2) correspond respectively to the gravity and the planing force. $R_c$ is the cavitator radius and $R$ is the supercavitating body radius. The coefficients $a_{ij}$, $b_{ij}$, and $d_{ij}$ are functions of system parameters. The immersion depth $h'$ and the angle of attack $\alpha$ in the planing force calculation are given by

$$
h' = \begin{cases} 0 & \frac{R_c-R}{R} > \frac{L|w|}{RV} \\ \frac{L|w|}{RV} - \frac{R_c-R}{R} & \text{otherwise} \end{cases} \quad (3)
$$

$$
\alpha = \begin{cases} \frac{w-\dot{R}_c}{V} & \frac{w}{V} > 0 \\ \frac{w+\dot{R}_c}{V} & \text{otherwise} \end{cases} \quad (4)
$$

In Eq. (3) and (4), $L$ is the vehicle length and $\dot{R}_c$ is the cavity radius contraction rate. The coefficients and other quantities above in Eqs. (2-4) take the forms given in Eq. (5). Here, $n$ is the fin effectiveness ratio with respect to the cavitator, $m$ is the density ratio of the body to water, $g$ is the gravity acceleration, $C_{x0}$ is the cavitator lift force coefficient, and

$R_n$ is the cavitator radius.

$$
a_{22} = \frac{CVT}{m}(\frac{-1-n}{L})S + \frac{17}{36}nL
$$
$$
a_{24} = VTS(C\frac{-n}{m}+\frac{7}{9}) - VT(C\frac{-n}{m}+\frac{17}{36})\frac{17}{36}L^2
$$
$$
a_{42} = \frac{CVT}{m}(\frac{17}{36} - \frac{11n}{36})
$$
$$
a_{44} = \frac{-11CVTnL}{36m}
$$
$$
b_{21} = \frac{CV^2Tn}{m}(\frac{-S}{L}+\frac{17L}{36}), \quad b_{22} = \frac{-CV^2TS}{mL}
$$
$$
b_{41} = \frac{-11CV^2Tn}{36m}, \quad b_{42} = \frac{17CV^2T}{36m} \quad (5)
$$
$$
c_2 = g, \quad d_2 = \frac{T}{m}(\frac{-17L}{36}+\frac{S}{L}), \quad d_4 = \frac{11T}{36m}
$$
$$
S = \frac{11}{60}R^2 + \frac{133L^2}{405}, \quad T = \frac{1}{7S/9 - 289L^2/1296}
$$
$$
C_x = C_{x0}(1+\sigma), \quad C = 0.5C_x\frac{R_n^2}{R^2}
$$
$$
R_c = R_n\sqrt{0.82\frac{1+\sigma}{\sigma}}K_2, \quad K_1 = \frac{L}{R_n(\frac{1.92}{\sigma}-3)} - 1
$$
$$
K_2 = \sqrt{1-(1-\frac{4.5\sigma}{1+\sigma})K_1^{40/17}}
$$
$$
\dot{R}_c = \frac{-\frac{20}{17}(0.82\frac{1+\sigma}{\sigma})^{0.5}V(1-\frac{4.5\sigma}{1+\sigma})(K_1)^{23/17}}{K_2(\frac{1.92}{\sigma}-3)}
$$

The model equations described here are different from that presented in reference [1], since the same sign convention is used for the cavitator and fin inputs. The planing force is the only nonlinearity considered in this work. Additional details regarding this model can be found in references [1] and [3].

## III. SYSTEM DYNAMICS

Results obtained for a representative set of system-parameter values are presented and discussed here. (A more complete discussion of the system behavior for different parameter values can be found in reference [3].) The specific set of parameter values considered is as follows: $g = 9.81m/s^2, m = 2, R_n = 0.0191m, R = 0.0508m, L = 1.8m, V = 75m/s, \sigma = 0.03, n = 0.5, C_{x0} = 0.82$.

### A. Time-Domain Simulations

The responses of the uncontrolled system were found to be unstable [3]. Responses of the controlled system are studied for the feedback law given by Eq. (6) and the results are presented in Fig. 2. As shown in this figure, the controlled system exhibits bounded motions, which happen to be stable periodic motions.

$$
\delta_c = -k_{21}z - k_{23}\theta - k_{24}q = 15z - 30\theta - 0.3q
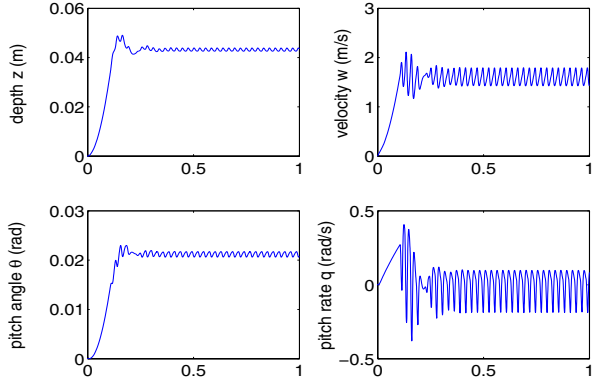$$
$$
\delta_e = 0 \quad (6)
$$

Fig. 2. Motions initiated from trivial initial conditions in the controlled case.
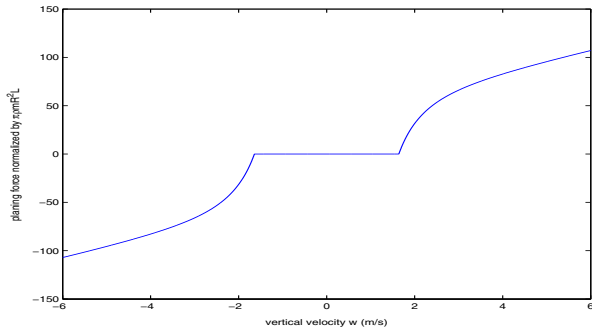


Fig. 3. Planing force versus the vertical speed $w$.

### B. Equilibrium-Point Analysis

A graph of the planing force is shown in Fig. 3. This nonlinearity depends only on the vertical speed w. Based on the w value, the state space can be divided into two regions; that is, the no-tail-slap region ($-w_0 < w < w_0$) and the tail-slap region ($|w| > w_0$), where $w_0$ is the positive value of $w$ at the transition point in Fig. 3. In the no-tail-slap region, the planing force is absent and the system is linear. The uncontrolled system has no equilibria in either region. The closed-loop system with the control given by Eq. (7) has the following numerically determined equilibrium point:

$$(\bar{z}, \bar{w}, \bar{\theta}, \bar{q}) = (0.04545, 1.6703, 0.0224, 0) \qquad (7)$$

The Jacobian matrix associated with this equilibrium point has unstable eigenvalues, and the DC offsets of the different states shown in Fig. 2 correspond to this unstable equilibrium point.

### C. Limit Cycle Prediction Using the Describing Function Method

To examine the limit cycle motions shown in Fig. 2, the describing function method (DFM) is used. This method, which is also known as the harmonic balance method, is a very useful tool in nonlinear system analysis [6], [7]. Through numerical calculations [3] based on this method, it

is determined that the system has a stable limit cycle with the vertical speed

$$w(t) = 1.626 + 0.12238 \cos(277t) \qquad (8)$$

The DC offset of 1.626 m/s is in agreement with the DC offset of 1.619 m/s determined through time-domain simulations (see Figure 2). In addition, the AC amplitude of 0.12238 m/s and the oscillation frequency of 277 rad/s are close to the respective values (0.2 m/s and 232 rad/s) obtained through the simulations. The differences are attributed to the presence of higher order harmonics; it is assumed that the first harmonic is dominant in using the DFM. A projection of the system trajectory obtained through the time-domain simulation is shown in Fig. 4.
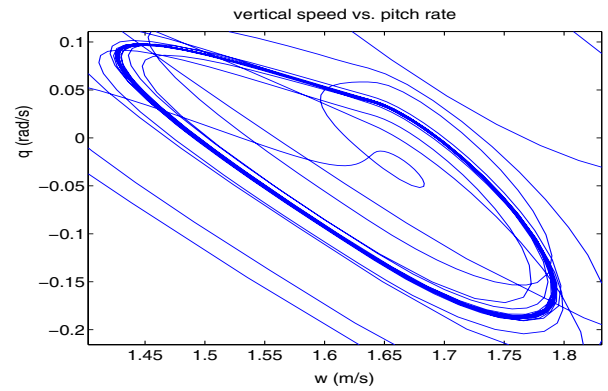


Fig. 4. Projection of the system trajectory obtained from time-domain simulations in the controlled case.

## IV. BIFURCATION ANALYSIS

In Section III, the solution structure of the system (2) was discussed for a selected set of parameter values. To fully understand the dynamics of the non-smooth system, it is important to determine the qualitative changes (bifurcations) experienced by the solutions of the system as a control parameter such as the cavitation number is varied. Different possible bifurcations include saddle-node bifurcation of a fixed point, pitchfork bifurcation of a fixed point, transcritical bifurcation of a fixed point, Hopf bifurcation of a fixed point, and period-doubling bifurcation of a periodic solution [5]. In order to determine a valid range of the cavitation number that would be physically meaningful, some analysis is needed, as discussed next.

### A. Physically Meaningful Range of the Cavitation Number

In previous studies ([1], [3], [8]), the operating cavitation number of the supercavitating vehicle is chosen as $\sigma = 0.03$. The model given by Eqs. (2-4) is valid only for cases with supercavitation. However, a large cavitation number corresponds to the no-cavity case or a partial-cavity case. On the other hand, a very small cavitation number is not practical due to the physical constraints, such as the vehicle speed. Furthermore, the assumptions made in deriving and

simplifying the cavity model lead to additional constraints on the cavitation number. An inspection of the cavity model (see Eq. (5)) reveals the following three constraints on the cavitation numbers:

1) $K_1 > 0 \Rightarrow \sigma > 0.0198$
2) $1 - (1 - \frac{4.5\sigma}{1+\sigma})K_1^{40/17} \Rightarrow \sigma < 0.0398$
3) $R_c > R \Rightarrow \sigma < 0.0368$

The expressions of the cavity radius $R_c$ at the transom, the planing section, and its derivative in Eq. (5) are simplified forms that follow from Logvinovich's cavity model [8]. The first constraint follows directly from the assumption

$$L > R_n(\frac{1.92}{\sigma} - 3) \qquad (9)$$

made during the simplification, which one can notice from the definition of the constant $K_1$. The second constraint is enforced to ensure that the cavity radius expression of Logvinovich's model has a real value at the body's transom [8]. The third constraint allows for the cavity to have a larger radius than the body at the transom. Hence, based on this discussion, the simplified cavity model is applicable only when the cavitation number falls within the interval [0.0198, 0.0368].

### B. Smooth Approximation of the Model

Due to the non-smooth nature of the system, it is not feasible to determine the fixed points of the given dynamic system and the bifurcations of these fixed points. Hence, one has to resort to numerical bifurcation analysis tools. Although bifurcation packages such as BIFPAK and Slide-Cont [9] are available for non-smooth systems, the nature of the non-smooth system (2) does not lend itself to the use of these tools.

The sources of non-smoothness in the planing force are the angle of attack $\alpha$ and the immersion depth $h'$. The equations governing the angle of attack given in Eq. (4) can be rewritten as

$$\alpha = \frac{w}{V} - \frac{|w|\dot{R}_c}{wV} = \frac{w}{V} - sgn(w)\frac{\dot{R}_c}{V} \qquad (10)$$

where $sgn(.)$ is the sign function that takes the form

$$sgn(x) = \begin{cases} 1 & \text{if } x > 0 \\ 0 & \text{if } x = 0 \\ -1 & \text{if } x < 0 \end{cases} \qquad (11)$$

The equations governing the immersion depth are provided in Eq. (3).

In Fig. 5 and 6, graphs of the angle of attack and the immersion depth are provided with respect to the vertical speed $w$. It is clear from Eqs. (10)-(12) as well as the graphs that the angle of attack and the immersion depth are piecewise linear functions of the vertical speed.

Based on prior work (e.g., [10]), hypertangent functions are chosen to obtain smooth versions of Eqs. (10) and (12). In the expression for the angle of attack, the $sgn(w)$ function is replaced by $tanh(kw)$, where $k$ is a constant chosen to
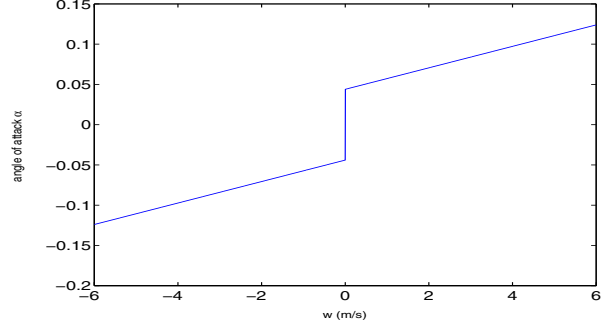


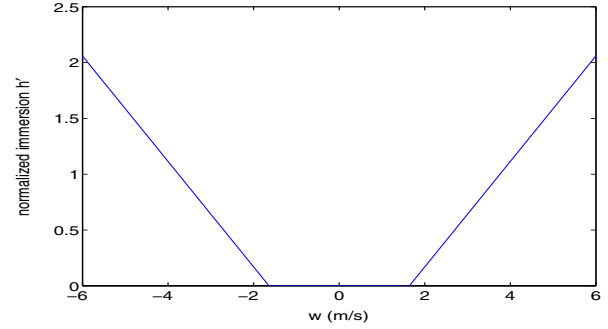Fig. 5. Angle of attack versus the vertical speed $w$.



Fig. 6. Immersion depth versus the vertical speed $w$.

control the approximation error. The immersion depth $h'$ is approximated as

$$h' \approx \tanh(kw)\frac{L}{2RV}f(w)$$
$$f(w) = 2w + (w + w_{t0})\tanh[-k(w + w_{t0})] \qquad (12)$$
$$+ (w - w_{t0})\tanh[k(w - w_{t0})]$$

In Eq. (12), $w_{t0}$ is the positive value of $w$ at the transition point in Fig. 6. In Fig. 7 and 8, comparisons between the smoothened version of the planing force and the non-smooth planing force are shown for two different values of $k$. It is clear that as the value of $k$ is increased, the approximation gets better. This is to be expected, since the non-smooth expressions are approached in the limit by the respective smooth approximations, as $k$ goes towards infinity. For $k = 300$ and beyond, the bifurcation results presented in the next section did not change from one value of $k$ to a higher one.

### C. Bifurcation Results

Since the uncontrolled system did not have any equilibrium points in the considered range of the cavitation number, bifurcations of equilibrium points of the smooth version of the controlled system were studied by using AUTO97. The control law given by Eq. (6) was used. The results are shown in Fig. 9. The solid thick line corresponds to stable limit cycles, solid thin lines correspond to stable
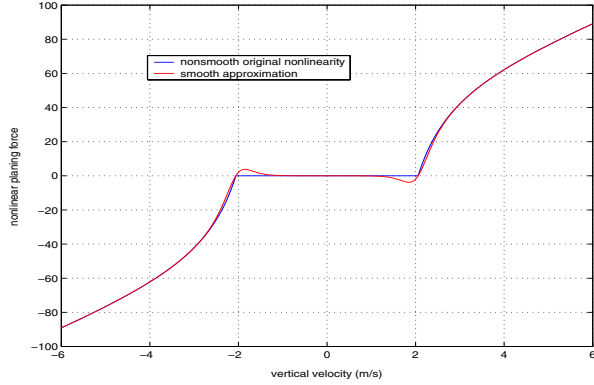
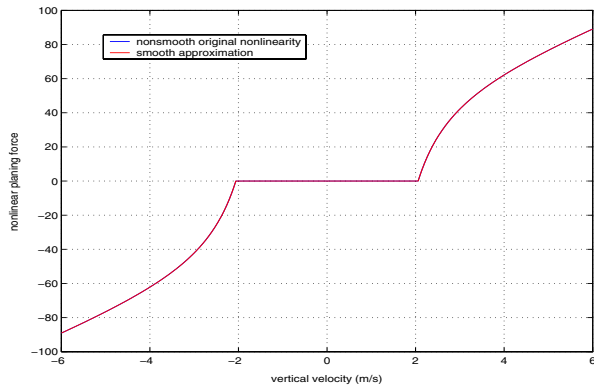Fig. 7. Comparisons between smooth form ($k = 3$) and non-smooth form.



Fig. 8. Comparisons between smooth form ($k = 300$) and non-smooth form.
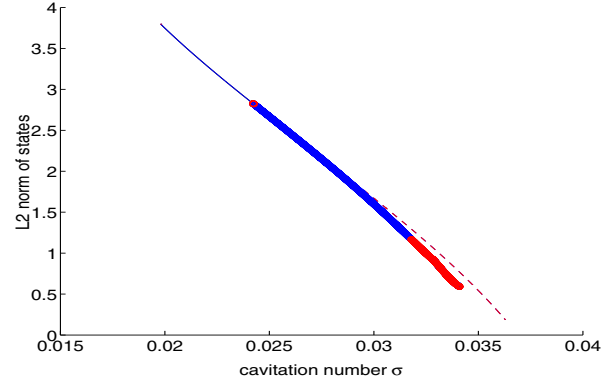


Fig. 9. Bifurcation diagram of the smooth system when the cavitation number is used as a control parameter.



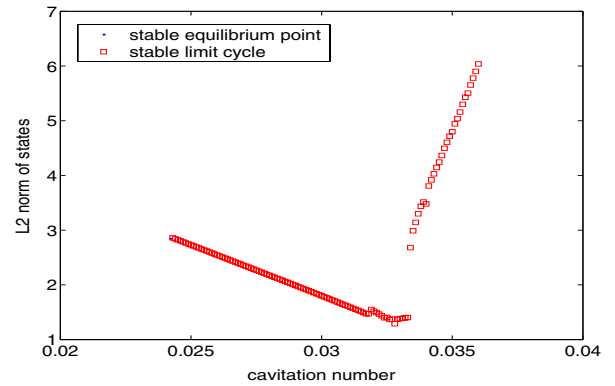Fig. 10. Steady solution of the non-smooth system when the cavitation number is used as a control parameter.

equilibrium points, and dotted thin lines correspond to unstable equilibrium points. A supercritical Hopf bifurcation occurs at $\sigma = 0.02425$. The numerical results also show that there are period-doubling bifurcations at the cavitation number values of 0.0318 and 0.0328.

To verify the results obtained by using AUTO97, the stability of the fixed point of the non-smooth system was numerically examined at the Hopf bifurcation point. It was numerically determined that the conditions required for a Hopf bifurcation of a fixed point including the transversality condition was satisfied. To verify the occurrence of a supercritical Hopf bifurcation of the fixed point of the non-smooth system, numerical simulations were carried out and the results obtained are presented in Fig. 10. The results confirm the existence of a supercritical Hopf bifurcation at a cavitation number value between 0.0242 and 0.0243 and possibly another bifurcation between the cavitation numbers of 0.0333 and 0.0334. It is believed to be related to the period-doubling bifurcation of the smooth version.

## V. BIFURCATION CONTROL

Typically, in bifurcation control (e.g., [11]), the uncontrolled system exhibits a bifurcation which one seeks to delay or suppress by choosing an appropriate feedback control law. Here, the bifurcation diagram shown in Fig. 9 pertains to a certain choice of coefficients in the control law given by Eq. (6). These coefficients are varied to shift the Hopf bifurcation of the fixed point. For the control law given by

$$\delta_e = 0, \delta_c = 15z - 300\theta - 3q \qquad (13)$$

the Hopf bifurcation point is delayed till the cavitation number is increased to a value of $\sigma = 0.03456$. This would mean that the motions of the supercavitating body will settle down to the stable equilibrium point solution for the values of $\sigma$ in the range of [0.0198, 0.03456]. For the choice of the control law

$$\delta_e = 0, \delta_c = 15z - 30\theta - 6q \qquad (14)$$

there are no Hopf bifurcations in the physically meaningful range of the cavitation number.

With the feedback control law

$$\delta_e = 0, \delta_c = 15z - 3000\theta - 0.3q \qquad (15)$$

the Hopf bifurcation point occurs at $\sigma = 0.0215$, which is earlier than that observed in Fig. 9. From a physical standpoint, usually the tail-slap is harmful to the supercavitating

body and these results suggest that the tail-slap behavior (associated with limit-cycle motions) can be eliminated by the choice of appropriate feedback control laws. Alternatively, if this behavior is preferred, the feedback control law can be used to enable this as well.

## VI. Concluding Remarks

The dive plane dynamics of the supercavitating body is modeled by using a non-smooth continuous differential system. The describing function method is used to predict limit cycle solutions and the results are shown to agree with previous work.

The change of the supercavitating body dynamics is studied as the cavitation number, a key parameter in supercavitation, is varied in an appropriate range. The non-smooth system is smoothened for bifurcation analysis. Hopf bifurcations of fixed points are found and the occurrence of these bifurcations are delayed or triggered earlier by using linear feedback control. The bifurcation results obtained for the smooth approximation of this system are also compared with those obtained for the original non-smooth system. Agreement is found in Hopf bifurcation values for a range of cavitation numbers. However, at a high value of the cavitation number, the results obtained from the two systems do not match well, possibly due to the complicated non-smooth dynamics of the original system.

## References

[1] J. Dzielski and A. Kurdila, "A benchmark control problem for supercavitating vehicles and an initial investigation of solutions," *Journal of Vibration and Control*, vol. 9, no. 7, pp. 791–804, 2003.

[2] I. Kirschner, D. C. Kring, A. W. Stokes, N. E. Fine, and J. S. Uhlman, "Control strategies for supercavitating vehicles," *Journal of Vibration and Control*, vol. 8, pp. 219–242, 2002.

[3] G. Lin, B. Balachandran, and E. Abed, "Dynamics and control of supercavitating bodies," in *Proceedings of ASME IMECE2004*, Anaheim, California, November 2004.

[4] W. Kang and F. A. Papoulias, "Bifurcation and control of submersible vehicles with dive plane reversal," *Latin American Applied Research– an International Journal*, vol. 31, no. 3, pp. 141–148, 2001.

[5] A. H. Nayfeh and B. Balachandran, *Applied Nonlinear Dynamics*. John Wiley and Sons, 1994.

[6] A. Tesi, E. H. Abed, R. Genesio, and H. O. Wang, "Harmonic balance analysis of period-doubling bifurcations with implications for control of nonlinear dynamics," *Automatica*, vol. 32, no. 9, pp. 1255–1271, 1996.

[7] A. Gelb and W. E. V. Velde, *Multiple-input Describing Functions and Nonlinear System Design*. McGraw-Hill, 1968.

[8] A. J. Kurdila, R. Lind, J. Dzielski, A. Jammulamadaka, and A. Goel, "Dynamcs and control of supercavitating vehicles (draft, reference and user manual)," University of Florida, Gainesville, FL, Tech. Rep., 2003.

[9] F. Dercole and Y. A. Kuznetsov, "Slidecont: An auto97 driver for bifurcation analysis of filippov systems," *ACM Transactions on Mathematical Software*, 2004.

[10] H. Wolf, J. Kodvanj, and S. Bjelovucic-Kopilovic, "Effect of smoothing piecewise-linear oscillators on their stability predictions," *Journal of Sound and Vibration*, vol. 270, pp. 917–932, 2004.

[11] E. H. Abed, H. O. Wang, and A. Tesi, "Control of bifurcations and chaos," in *The Control Handbook*, W. S. Levine, Ed. CRC Press, 1996, pp. 951–966.